Plant Physiology, 2026, 201, 1–13
https://doi.org/10.1093/plphys/kiag454
Published: 29 June 2026
Research article

Plant Physiology®

H_2O_2 oxidation of VvMYB APL reduces *VvHSP20-43* expression and promotes grape ripening

Jia-Lin Xing[1,2‡], Lu Yang[1,2‡], Ding-Ding Zuo[2,3‡], Rui-Ya Li[3], Meng-Ling Zheng[1,2], Jing Zhang[1,2], Hai-Nan Liu[1,2], Mao-Song Pei[1,2], Tong-Lu Wei[1,2], Arif Atak[4], Justin G. Lashbrooke[5], and Da-Long Guo[1,2*]

[1]College of Horticulture and Plant Protection, Henan University of Science and Technology, Luoyang, Henan 471023, China
[2]Henan Key Laboratory of Germplasm Innovation and Utilization of Eco-Economic Woody Plant, Henan University of Science and Technology, Luoyang, Henan 471023, China
[3]College of Agronomy/Tree Peony, Henan University of Science and Technology, Luoyang, Henan 471023, China
[4]Department of Horticulture, Faculty of Agriculture, Bursa Uludağ University, Bursa 16059, Türkiye
[5]Department of Genetics, Stellenbosch University, Stellenbosch 7600, South Africa

*Corresponding author: Da-Long Guo, College of Horticulture and Plant Protection, Henan University of Science and Technology, Luoyang 471023, China. Email: guodalong@haust.edu.cn
‡These authors contributed equally to this work.
The author responsible for distribution of materials integral to the findings presented in this article in accordance with the policy described in the Instructions for Authors (https://academic.oup.com/plphys/pages/General-Instructions) is: Da-Long Guo.

Abstract

Previous studies have shown that hydrogen peroxide (H_2O_2) treatment promotes early ripening in "Kyoho" grapes (*Vitis vinifera* × *Vitis labrusca*); however, the mechanism by which H_2O_2 oxidation modification regulates grape ripening remains unclear. Here, RNA-Seq data revealed substantial downregulation of small Heat Shock Protein 20-43 (*VvHSP20-43*) expression levels in the treated group. Co-expression network analysis identified MYB Altered Phloem Development (VvMYB APL) as a key regulator of *VvHSP20-43* expression. Dual luciferase, yeast one-hybrid, and electrophoretic mobility shift assays confirmed that VvMYB APL binds to the *VvHSP20-43* promoter, thereby activating its transcriptional expression. Stable transformation in *Arabidopsis* and transient transformation in grape berries demonstrated that *VvMYB APL* and *VvHSP20-43* negatively regulate fruit ripening. Further analysis revealed that exogenous H_2O_2 treatment rapidly oxidizes the VvMYB APL protein, inducing methionine (Met) site mutations that inhibit its transcriptional activation of *VvHSP20-43*. In addition, reduced expression of *VvMYB APL* and *VvHSP20-43* promoted the expression of ripening-related genes, thereby accelerating grape berry ripening. This study elucidates the molecular mechanism by which H_2O_2 oxidizes the VvMYB APL transcription factor, thereby downregulating *VvHSP20-43* expression and influencing fruit ripening.

Introduction

Grape (*Vitis vinifera* L.) is a major cultivated fruit crop globally, typically classified into table grape and wine grape production, exhibiting a range of berry flavors, shapes, and colors (Di Genova et al. 2014; Torres-Palazzolo et al. 2024). In addition to being consumed fresh, grapes are widely processed into a variety of products such as wine, juice, and dried or preserved fruit (Almanza-Oliveros et al. 2024). Currently, most commercially cultivated table grape varieties are mid-ripening to late-ripening types, with production concentrated in a narrow harvest window (Segade et al. 2013; Atak 2024; Atak et al. 2025).

Fruit or berry ripening is a highly coordinated and complex regulatory process that is regulated by hormones, transcription factors (TF) and involving a variety of physiological and biochemical changes (Kumar et al. 2016; Steelheart et al. 2022; Zuo et al. 2025). The effect of ROS (such as H_2O_2) on fruit development has been found to be concentration-dependent, with low concentrations promoting development, whereas high concentrations exerted detrimental effects (Quan et al. 2008; Liao et al. 2012). While the positive regulatory role of H_2O_2 in the ripening process of both climacteric and nonclimacteric fruits has been observed, the regulatory mechanism of H_2O_2 was not fully understood (Yang et al. 2025).

H_2O_2 acts as an exogenous reactive oxygen species with oxidative properties, inducing oxidative modifications. This oxidative modification is a post-translational modification of a protein that depends on the oxidative ability of H_2O_2, similar to ubiquitination and phosphorylation (Wang et al. 2021). H_2O_2 can oxidize redox-sensitive cysteine (Cys) residues and Met residues on target proteins, thereby affecting the activity of many enzymes and TFs to regulate fruit ripening (Zhu et al. 2023). In tomatoes, H_2O_2 mediates the oxidation of Met-138 in

Received: July 3, 2025. **Accepted:** May 14, 2026
© The Author(s) 2026. Published by Oxford University Press on behalf of American Society of Plant Biologists. All rights reserved. For commercial re-use, please contact reprints@oup.com for reprints and translation rights for reprints. All other permissions can be obtained through our RightsLink service via the Permissions link on the article page on our site—for further information please contact journals.permissions@oup.com.

Downloaded from https://academic.oup.com/plphys/article/201/3/kiag454/8721702 by Uladag University user on 14 July 2026

NOR and regulates fruit ripening by reducing its DNA-binding capacity and in vitro transcriptional regulation activity (Jiang et al. 2020). In addition, banana EIL9 undergoes sulfoxidation at Met-129, −130, and −282 sites due to ROS accumulation, resulting in a decrease in its DNA-binding ability. While Met sulfoxide reductase A (MaMsrA4) can reduce the oxidized MaEIL9, restoring its activation ability for starch degradation genes such as *MaAMY3D* and *MaBAM1*, thereby promoting fruit ripening (Zhu et al. 2023). However, it is unknown whether the protein oxidation modification caused by H_2O_2 is involved in the ripening process of grape berries.

Grapes are a typical nonclimacteric fruit, and their ripening process can be significantly influenced by H_2O_2. Recent work has shown that H_2O_2 priming enhances the responsiveness of grape berries to subsequent stimuli by inducing alternative splicing changes and establishing splicing memory (Zuo et al. 2024). This is likely due to the involvement of H_2O_2 as a signaling molecule in the regulation of many ripening-related enzymes and TFs. Small heat shock proteins in plants are known as HSP20s due to their molecular weight ranging from 12 to 42 kDa (Van Montfort et al. 2001). They have been found to be differentially expressed after H_2O_2 treatment in grapes; they are also thought to be involved in fruit ripening (Guo et al. 2019; Ji et al. 2019; Guo et al. 2020). In tomatoes, the silencing of the *SlHSP17.7* gene leads to the downregulation of genes related to glucose metabolism and inhibits fruit ripening (Liu et al. 2023). RNA-Seq analysis revealed that 4 differentially expressed sHSP played an important role in the fruit development of "Heinz 1706" tomatoes (Arce et al. 2016). Based on the above results, it is concluded that the *HSP20* participates in the ripening process of fruit. However, the mechanism by which H_2O_2 affects the *HSP20s* to regulate fruit ripening remains unclear.

The effect of ROS on gene expression can be mediated by its regulation of redox-sensitive transcription factors, including MYB factors MYB30 and MYB111L (Mabuchi et al. 2018; Yao et al. 2020). While MYB transcription factors have been shown to play an important role in fruit development and ripening (Jin et al. 2016). In this study, we revealed the molecular mechanism by which the VvMYB APL protein was oxidized by H_2O_2 to regulate *VvHSP20-43* expression in grape berries. Furthermore, VvMYB APL regulates the expression of *VvHSP20-43* and negatively regulates fruit development. This work reveals regulatory mechanisms governing fruit development and ripening, providing a theoretical foundation for regulating grape ripening.

Results

VvHSP20-43 is localized to the cytoplasm and nucleus and responds to H_2O_2 signals

Grape berries exhibit distinct changes in size and color during development (Fig. 1a). In the early developmental stages (K1 and K2), the berries are pea-sized. The second developmental stage (K3) features berries that are touching. The third developmental stage (K4) features firm green berries. During the fourth stage (K5), berries begin to soften. In the fifth stage (K6), berries initiate color development (Wei et al. 2025). To explore the role of the *VvHSP20-43* gene in the development and ripening process of grape berries, the expression level of the *VvHSP20-43* gene in the fruits of "Kyoho" grapes under natural development conditions was determined. The results showed that the expression level of *VvHSP20-43* was lowest during the color change stage of grape berries and reaches its peak at ripening (Fig. 1b). It indicated that the *VvHSP20-43* gene plays a role before and after the color change period of grape berries.

Amino acid sequence analysis showed that there was a conserved PfamHSP20 domain in VvHSP20-43 (Fig. 1c). Subcellular localization results showed that VvHSP20-43 localized to the cytoplasm and nucleus of tobacco leaves (Fig. 1d). Histochemical staining of grape leaves using the *proVvHSP20-43*:GUS construct revealed that, in the presence of H_2O_2, the staining intensity of the *VvHSP20-43* promoter was reduced compared with the untreated control group (Fig. 1e). The same results were observed in tobacco leaves (Figure S1).

VvHSP20-43 inhibits fruit ripening

Stable overexpression of *VvHSP20-43* in *Arabidopsis* exhibited a late-ripening phenotype in their fruit pods (Fig. 2a). In addition, the overexpression of *VvHSP20-43* resulted in a delay of about 4 days in the ripening of *Arabidopsis* pods (Fig. 2b). To further explore the function of *VvHSP20-43* in the grape ripening process, the pIR-*VvHSP20-43* overexpression vector (pIR-*VvHSP20-43*-OE) and the pIR-*VvHSP20-43* silencing vector (pIR-*VvHSP20-43*-RNAi) were constructed, and the pIR empty vector was used as the control. Transgenic results indicate that compared with the pIR empty vector, grape berries injected with the pIR-*VvHSP20-43*-RNAi plasmid exhibited the early ripening phenotype, while berries injected with the pIR-*VvHSP20-43*-OE plasmid showed the delayed ripening phenotype (Fig. 2c). The results of fluorescence quantification demonstrated that a transient expression system had been successfully established in grape berries (Fig. 2d). During this period, by measuring the H_2O_2, anthocyanin, and sucrose content in grape berries, it was found that the H_2O_2, anthocyanin, and sucrose levels in grape berries injected with the pIR-*VvHSP20-43*-RNAi plasmid increased, whereas they decreased in berries injected with the pIR-*VvHSP20-43*-OE plasmid (Fig. 2e; Figure S2a and b). The results indicated that *VvHSP20-43* was a negative regulatory factor to regulate grape ripening.

The expression of ripening genes, such as ethylene-response element-binding factor (*VvERE*); anthocyanin biosynthesis-related genes, chalcone synthase (*VvCHS*), phenylalanine ammonia-lyase (*VvPAL*), MYB A1 transcription factor (*VvMYBPA1*); and other ripening-related genes, alcohol dehydrogenase 2 (*VvADH2*), AGAMOUS 2 (*VvAG2*), SEPALLATA3 (*VvSEP3*), and B-sister 1 (*VvBS1*), were investigated during the development and ripening of grape berries. The expression of them in pIR-*VvHSP20-43*-RNAi grape berries increased, and the expression of these genes in pIR-*VvHSP20-43*-OE grape berries decreased, contrary to the expression of *VvHSP20-43* (Fig. 2f).

VvMYB APL is the key transcription factor regulating *VvHSP20-43*

To further explore the regulatory mechanism of H_2O_2 treatment mediating the decreased expression of the *VvHSP20-43* gene, based on PlantTFDB, CIS-BD databases, and Plant TF Binding software in TBtools, the transcription factors that can bind to the promoter region of the *VvHSP20-43* gene were predicted (Table S1). The obtained results are intersected by the Veen diagram (Fig. 3a). Based on AlphaFold3, multiple VvMYB APL binding sites were identified in the promoter region of *VvHSP20-43* (Fig. 3b). GO enrichment analysis

Downloaded from https://academic.oup.com/plphys/article/201/3/kiag454/8721702 by Uladag University user on 14 July 2026

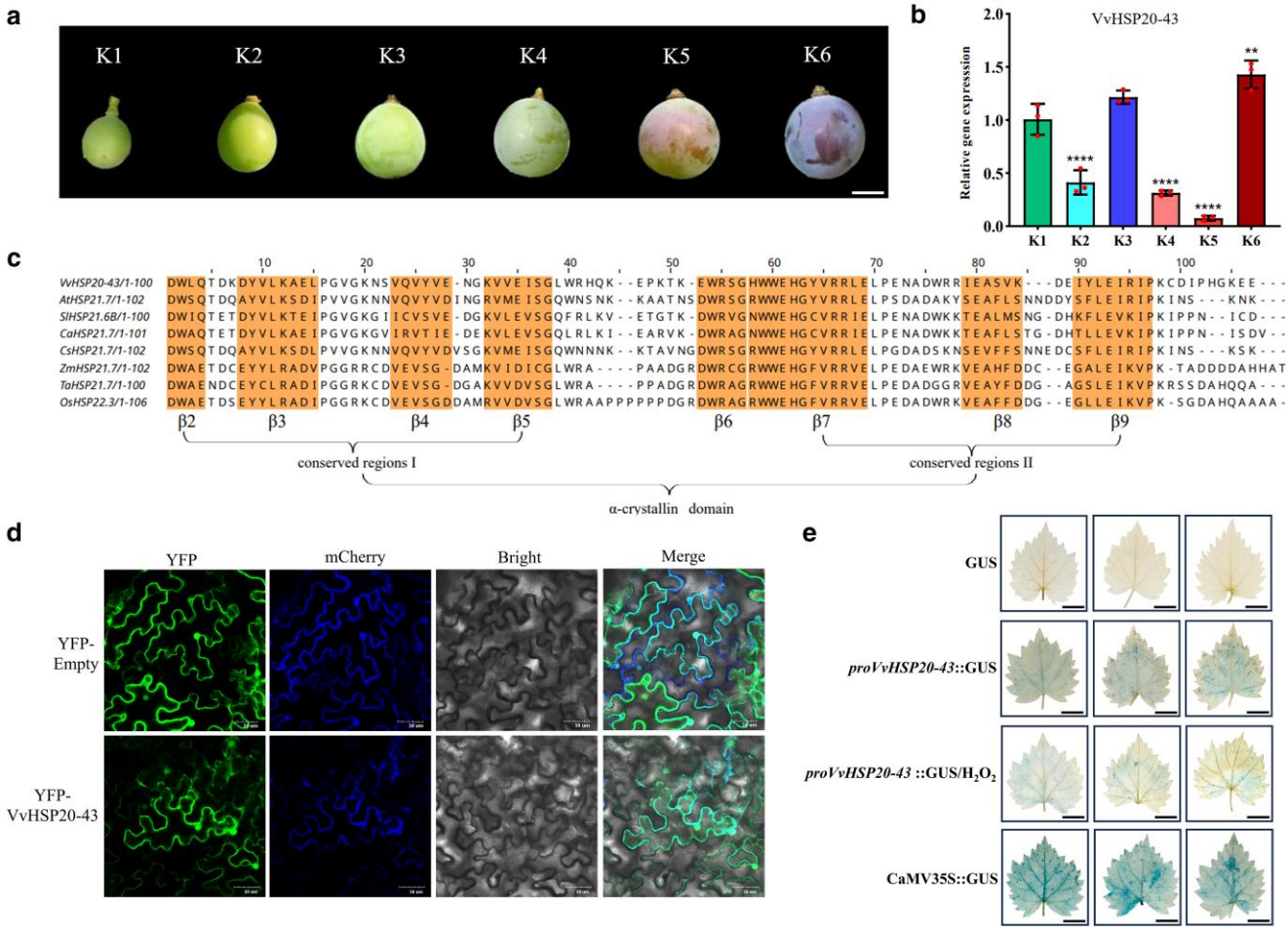


Figure 1 Identification of the H_2O_2-responsive *VvHSP20-43* gene in grape. a) Berry phenotypes of "Kyoho" at different developmental stages. K1 and K2: pea-size berries, K3: berry touching, K4: hard green berries, K5: starting to soften, K6: véraison. Images were digitally extracted for comparison. The scale bar is 1 cm. b) The expression level of the *VvHSP20-43* gene in "Kyoho" grapes under natural development conditions. Three independent biological replicates were analyzed for each treatment, and each biological replicate was measured using 3 technical PCR replicates. Data are presented as mean ± SD. c) Amino acid sequence analysis. d) Subcellular localization of VvHSP20-43 in *N. benthamiana* leaves. Using YFP empty as a positive control. The mCherry were used as cytoplasmic localization marker. Scale bar, 50 μm. e) Histochemical staining to analyze the promoter activity of *VvHSP20-43*. Using GUS empty as a negative control and CaMV35S::GUS as a positive control, with *proVvHSP20-43*::GUS subjected to treatments with 300 mmol/L H_2O_2. Images were digitally extracted for comparison. The scale bar is 1 cm. Three independent biological replicates were analyzed for each treatment. Data in (b) was analyzed by one-way ANOVA; significant differences were observed between the treatment group and the control group (*$0.01 < P < 0.05$, $0.001 <$ **$P < 0.01$, $0.0001 <$ ***$P < 0.001$, ****$P < 0.0001$). All *P*-values are shown in Data Set S2.

of 16 common TF genes showed that they were related to gene expression and plant development (Fig. 3c). Moreover, the expression patterns of these transcription factors were analyzed based on the transcriptome data of grape berries at different developmental stages after H_2O_2 treatment, to further identify the potent transcription factors regulating the *VvHSP20-43* gene (Fig. 3d).

VvMYB APL was identified as the most potent transcription factor in the process of H_2O_2 treatment-mediated *VvHSP20-43* gene expression reduction, based on the results of the grape co-expression network summarized from previous studies on grape microarray and transcriptome data (Wong 2020).

VvMYB APL is localized in the nucleus and responds to H_2O_2 signals

To further reveal the characteristics of *VvMYB APL*, we performed sequence analysis, subcellular localization, and promoter activity analysis of the *VvMYB APL* gene. Amino acid sequence analysis showed that there were 2 conserved Myb domains in VvMYB APL (Figure S3a). The location of the *VvMYB APL* gene in plant cells was studied by constructing YFP-VvMYB APL vector. The results of subcellular localization showed that VvMYB APL was located in the nucleus of tobacco leaves (Fig. 4a). Further analysis examined the effect of H_2O_2 treatment on *VvMYB APL* expression. Results indicated that H_2O_2 treatment led to reduced expression of *VvMYB APL* (Fig. 4b and c). According to evolutionary analysis, VvMYB APL was highly homologous to AtMYB APL with similar conserved domains (Fig. 4d). *proVvMYB APL:*GUS vector was constructed, and histochemical staining was performed to analyze the promoter activity of *VvMYB APL*. The staining results of grape leaves showed that the promoter of the *VvMYB APL* can normally start the expression of *VvMYB APL* gene. And the staining intensity of the activity of *VvMYB APL* promoter was reduced by H_2O_2 (Fig. 4e). Similarly, the results were observed in tobacco leaves (Figure S3b).

Downloaded from https://academic.oup.com/plphys/article/201/3/kiag454/8721702 by Uladag University user on 14 July 2026

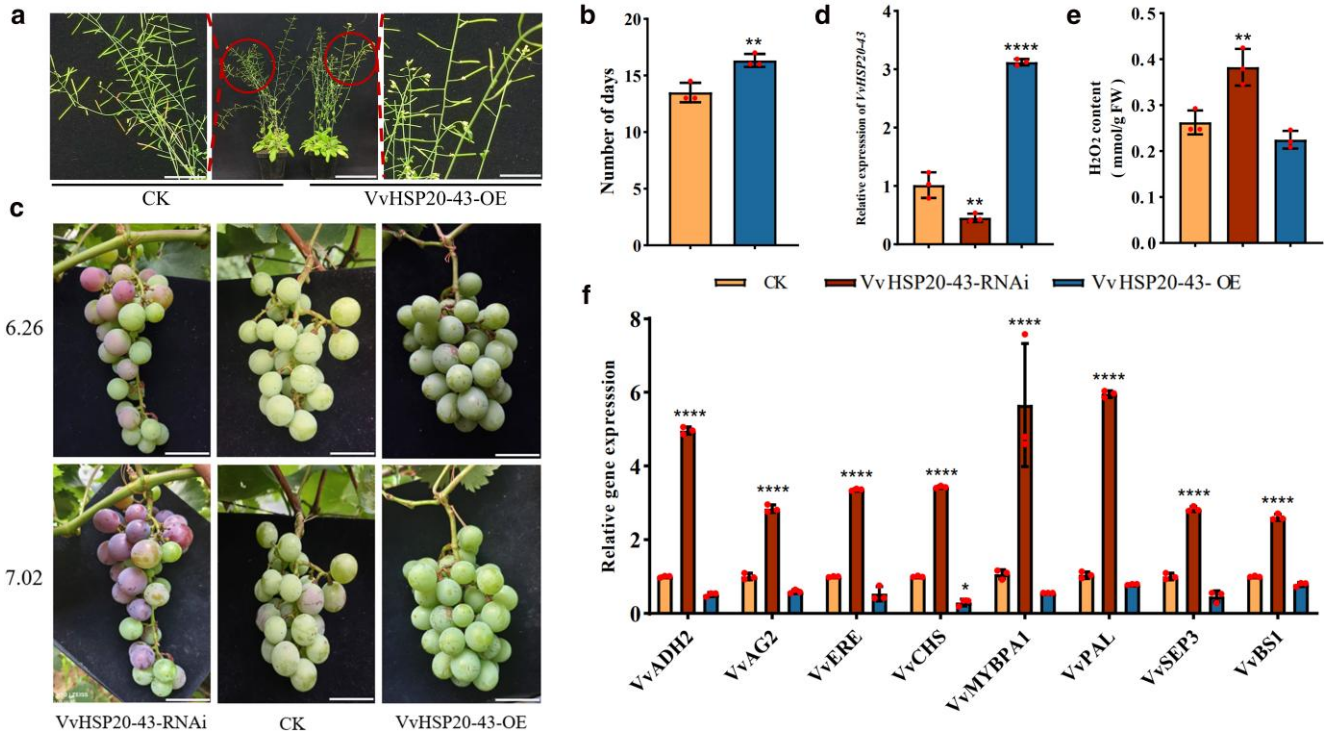


Figure 2 *VvHSP20-43* negatively regulates fruit ripening. a) Phenotypic observation of positive transgenic *Arabidopsis* plants expressing *VvHSP20-43*. CK: wild type plants serve as a control. Scale bar is 1 cm. b) The mature days of *Arabidopsis* fruit pods. Data are presented as means ± SD of 3 independent biological replicates ($n = 3$), representing 3 independent transgenic lines. c) Grape berry phenotypes transiently overexpressing or silencing *VvHSP20-43*. CK: pIR empty as control. Scale bar is 1 cm. d) The expression pattern of *VvHSP20-43* in transgenic berries. Three independent biological replicates were analyzed for each treatment, and each biological replicate was measured using 3 technical PCR replicates. Data are presented as mean ± SD. e) Analysis of H_2O_2 content of *VvMYB APL* in transgenic berries. FW, fresh weight. Data are presented as means ± SD of 3 independent biological replicates ($n = 3$). Each biological replicate consists of 3 grape clusters processed independently. f) Expression patterns of ripening-related genes in transgenic berries. Three independent biological replicates were analyzed for each treatment, and each biological replicate was measured using 3 technical PCR replicates. Data are presented as mean ± SD. Data in b), d) and e) were analyzed by one-way ANOVA; data in (**f**) was analyzed by two-way ANOVA. Significant differences were observed between the treatment group and the control group (*$0.01 < P < 0.05$, $0.001 <$ **$P < 0.01$, $0.0001 <$ ***$P < 0.001$, ****$P < 0.0001$). All *P*-values are shown in Data Set S2.

VvMYB APL inhibits fruit ripening

Stable overexpression of *VvMYB APL* in *Arabidopsis* exhibited a late-ripening phenotype (Fig. 5a). The overexpression of *VvMYB APL* resulted in a delay of days in the ripening of *Arabidopsis* pods (Fig. 5b). In addition, transgenic results indicate that compared with the pIR empty vector, grape berries injected with the pIR-*VvMYB APL*-RNAi plasmid exhibited early ripening, while berries injected with the pIR-*VvMYB APL*-OE plasmid showed delayed ripening (Fig. 5c). The results of fluorescence quantification demonstrated that a transient expression system had been successfully established in grape berries (Fig. 5d). During this period, by measuring the H_2O_2, anthocyanin, and sucrose content in grape berries, it was found that the H_2O_2, anthocyanin, and sucrose levels in grape berries injected with the pIR-*VvMYB APL*-RNAi plasmid increased, whereas they decreased in berries injected with the pIR-*VvMYB APL*-OE plasmid (Fig. 5e; Fig. S4a and b). The ripening genes (*VvERE*, *VvCHS*, *VvPAL*, *VvMYBPA1*, *VvADH2*, *VvAG2*, *VvSEP3*, and *VvBS1*) were associated with ripening during the development and ripening of grape berries. The expression of these genes in pIR-*VvMYB APL*-RNAi grape berries increased, and the expression of these genes in pIR-*VvMYB APL*-OE grape berries decreased (Fig. 5f). The results indicated that *VvMYB APL* is a negative regulator of grape ripening.

VvMYB APL binds to the *VvHSP20-43* promoter and activates its expression

Based on previous studies and biological information prediction results, *VvMYB APL* is a key transcription factor regulating *VvHSP20-43*. In order to confirm the regulatory role between them, a yeast one-hybrid assay was conducted based on AD-VvMYB APL and pBait-AbAi-*VvHSP20-43* plasmids. The results showed that the AbA concentration inhibiting the growth of pBait-AbAi-*VvHSP20-43* yeast strains was 300 ng/mL compared with the AD-Empty + pAbAi-*VvHSP20-43* promoter in the control group. The yeast strains of AD-VvMYB APL + pAbAi-*VvHSP20-43* coated on SD/-Leu with AbA are able to grow, indicating that VvMYB APL can bind to the *VvHSP20-43* promoter (Fig. 6a). In addition, the result was further confirmed by dual-luciferase reporter assays. In this study, we constructed a fusion of the *VvHSP20-43* promoter region (−930 bp to −1,522 bp) with the pGreenllo800-LUC vector, resulting in the *proVvHSP20-43*-LUC construct. Additionally, we fused the CDS of VvMYB APL to the pSAK277 vector, yielding the pSAK-VvMYB APL construct (Fig. 6b). The results of the dual-luciferase reporter assays showed that compared with the control group, pSAK277 + *VvHSP20-43*-LUC, the tobacco leaves injected with the mixture of *VvHSP20-43* and VvMYB APL showed fluorescence (Fig. 6c). The LUC

Downloaded from https://academic.oup.com/plphys/article/201/3/kiag454/8721702 by Uladag University user on 14 July 2026

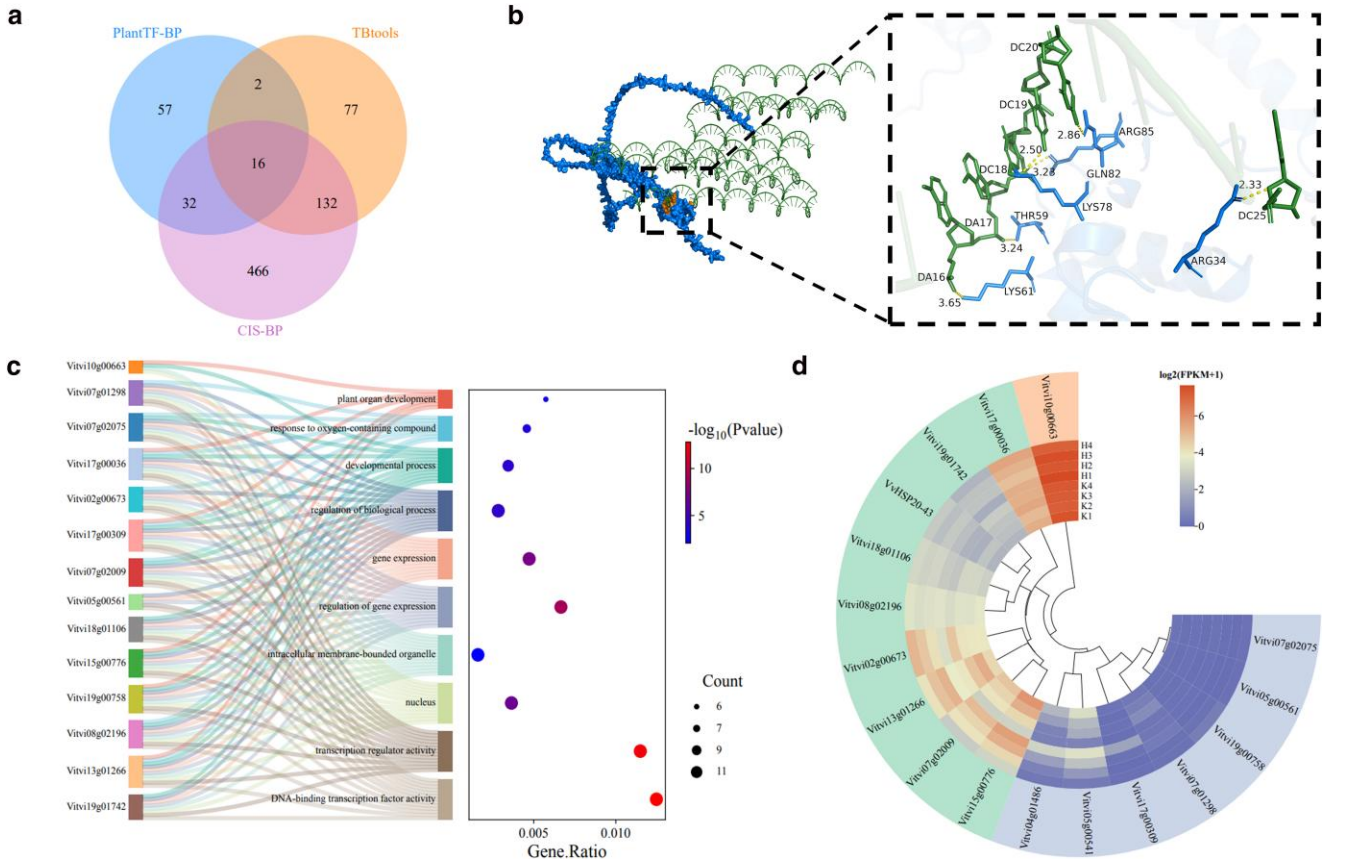


Figure 3 Identification of the candidate transcription factors regulating *VvHSP20-43*. a) Identification of candidate TFs for *VvHSP20-43*. b) Prediction of *VvHSP20-43* promoter and VvMYB APL protein interactions using AlphaFold3, visualized by PyMOL. The DNA fragment represents the *VvHSP20-43* promoter, and the protein model represents VvMYB APL. c) GO enrichment analysis of candidate TFs for *VvHSP20-43*. d) Expression pattern analysis of candidate TFs for *VvHSP20-43*. The heatmap scale represents relative expression levels.

value of tobacco leaves injected with *VvHSP20-43* and VvMYB APL was higher than that of tobacco leaves injected with pSAK277 + *VvHSP20-43*-LUC (Fig. 6d). The promoter of *VvHSP20-43* contains a Myb element (P1: −1,111 bp ~ −1,116 bp). We further performed an electrophoretic mobility shift assay (EMSA) on the VvMYB APL-MBP protein. The theoretical size of the recombinant protein with tags ranged from 80 to 90 KDa, and the expression of the purified protein conformed to the theoretical size of the protein with tags attached (Figure S5). The results showed that VvMYB APL-MBP specifically binds to the Myb element in the *VvHSP20-43* promoter (Fig. 6e). The intensity of the VvMYB APL protein complex bands diminished progressively as the concentrations of competing probes increased. In contrast, no complex bands were detected in the presence of competing probes when biotin-labeled mutant probes (where CAGTTA was altered to ACTGGC) were introduced. These findings strongly support the idea that the VvMYB APL-MBP protein binds specifically to the *VvHSP20-43* promoter through the Myb recognition sequence. Further treatment of the VvMYB APL protein with H_2O_2 and subsequent EMSA analysis revealed that the mutated VvMYB APL protein could no longer bind specifically to the *VvHSP20-43* promoter (Figure S6). The results showed that VvMYB APL can significantly activate the activity of the *VvHSP20-43* promoter, and VvMYB APL, as a transcriptional activator, can positively regulate the expression of *VvHSP20-43*.

Identification of VvMYB APL oxidation modification sites

Based on our previous results, it is speculated that H_2O_2 treatment may mediate the oxidative modification of the VvMYB APL protein. Firstly, multiple Met sites that are easily oxidized were identified by analyzing the amino acid sequence of VvMYB APL protein (Fig. 7a; Table S2). To investigate whether VvMYB APL can be oxidized by H_2O_2, the purified VvMYB APL protein was treated with H_2O_2, and then it was verified by liquid chromatography tandem mass spectrometry (LC-MS/MS) that the VvMYB APL protein could be oxidized by H_2O_2, and oxidative modification occurred at 2 Met sites of the VvMYB APL protein (Fig. 7b and c).

To further verify our hypothesis that the Met active site of VvMYB APL is modified by H_2O_2 oxidation, which changes its binding activity with *VvHSP20-43*, thus causing the differential expression of the *VvHSP20-43* gene. A dual-luciferase reporter assay was conducted, in which infected tobacco leaves were treated with H_2O_2 and then analyzed using in vivo imaging or quantitative fluorescence detection. The results indicate that H_2O_2 reduced reporter gene expression from the *VvHSP20-43* promoter. Furthermore, in the control group, VvMYB APL significantly activated the expression of the reporter gene driven by the *VvHSP20-43* promoter in tobacco leaves injected with the dual-gene construct. In contrast, in the H_2O_2-treated group, VvMYB APL underwent oxidative modification, which attenuated the transcriptional activation of the *VvHSP20-43* promoter by

Downloaded from https://academic.oup.com/plphys/article/201/3/kiag454/8721702 by Uladag University user on 14 July 2026

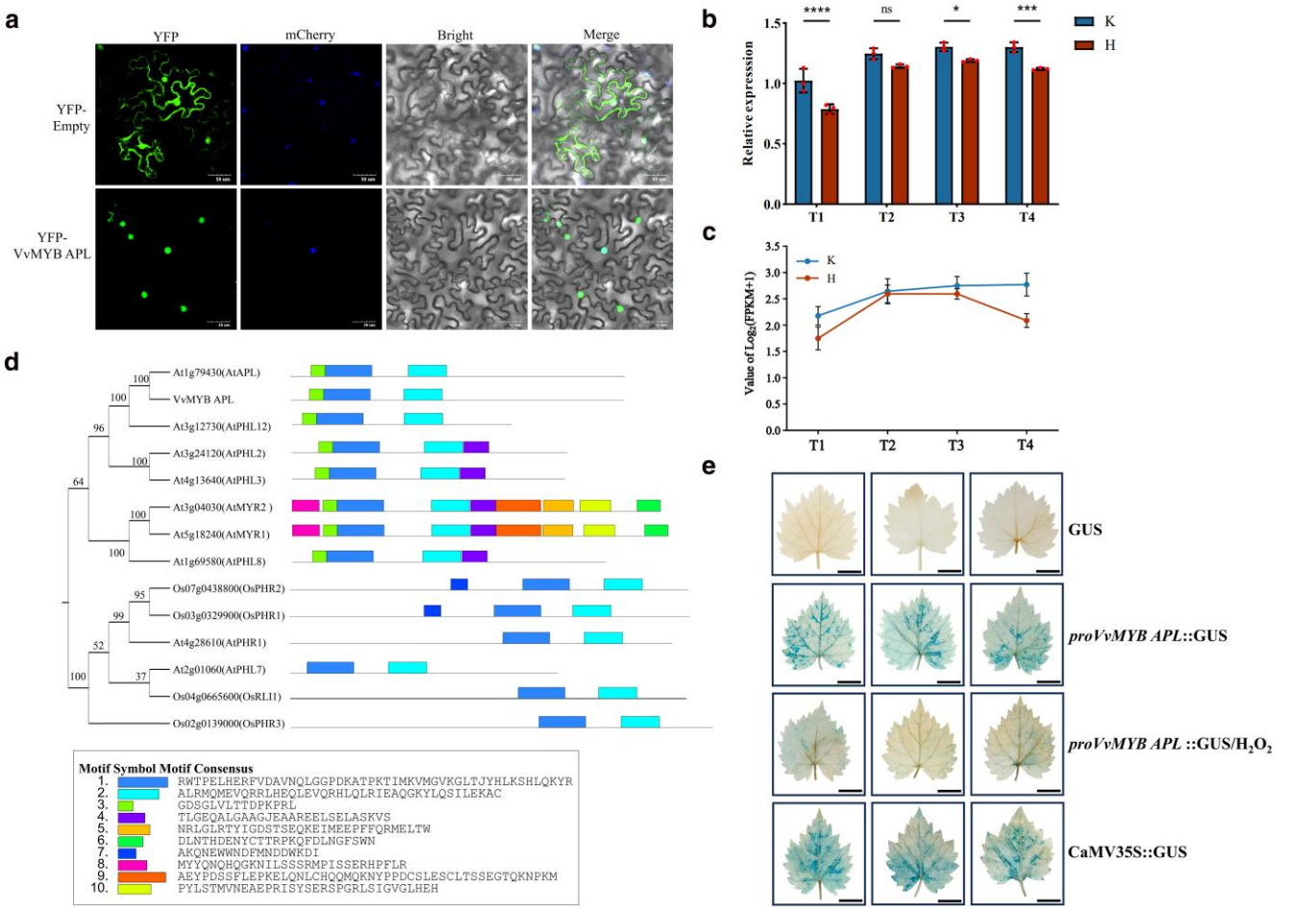


Figure 4 Identification of the H_2O_2-responsive *VvMYB APL* gene in grape. a) Subcellular localization of VvMYB APL in *N. benthamiana* leaves. Using YFP empty as a positive control. The mCherry was used as nuclear localization marker. Scale bar, 50 μm. b) RT-qPCR assay for relative expression of the *VvMYB APL*. Three independent biological replicates were analyzed for each treatment, and each biological replicate was measured using 3 technical PCR replicates. Data are presented as mean ± SD. c) Expression pattern analysis of *VvMYB APL*. The line chart depicts the expression levels within the *VvMYB APL* transcriptome. Samples were initially taken at 35 DAF and continued at 10-day intervals until treated berry reached ripening, resulting in 4 sampling time points designated as T1 through T4. H for H_2O_2-treated berries, K for untreated control berries. d) Phylogenetic tree analysis and motif analysis for MYB APL. Numbers at the nodes indicate bootstrap support values based on 1,000 replicates. e) Activity analysis of *VvMYB APL* promoter. Using GUS empty as a negative control and CaMV35S::GUS as a positive control, with *proVvMYB APL*::GUS subjected to treatments with 300 mmol/L H_2O_2. The scale bar is 1 cm. Three independent biological replicates were analyzed for each treatment. Images were digitally extracted for comparison. Data in b) was analyzed by two-way ANOVA. Significant differences were observed between the treatment group and the control group (*0.01 < *P* < 0.05, 0.001<**P* < 0.01, 0.0001<***P* < 0.001, ****P* < 0.0001). ns, no significance. All *P*-values are shown in Data Set S2.

VvMYB APL (Fig. 7d). Further mutations were introduced at 2 Met sites within the *VvMYB APL* coding sequence (Fig. 7e). Transient overexpression transformations were performed in grape berries. RT-qPCR analysis revealed that the normally expressed *VvMYB APL* was successfully overexpressed, whereas the mutated *VvMYB APL* was not overexpressed (Fig. 7f). Furthermore, *VvHSP20-43* expression levels increased in berries expressing the unmutated *VvMYB APL*, while no significant changes were observed in berries expressing the mutated *VvMYB APL* (Fig. 7g). The results indicated that the sulfoxidation of VvMYB APL weakens its ability to bind the *VvHSP20-43* promoter, thereby inhibiting transcriptional activation of *VvHSP20-43*.

Discussion

In our previous study, treating "Kyoho" grapes with H_2O_2 was found to promote early ripening (Guo et al. 2019). Transcriptome analysis showed that the expression of most of *VvHSP20s* genes decreased after treatment with H_2O_2 at 35, 45, 55, and 65 days after flowering (DAF). *VvHSP20s* genes are involved in the development of grapes, and *VvHSP20-43* gene expression levels were significantly different in each treatment period (Ji et al. 2019). Thus, *VvHSP20-43* is speculated to play an important role in H_2O_2-mediated fruit ripening. In plants, HSP20s, containing a highly conserved α-crystallin domain (ACD), are the most abundant and widely distributed heat shock proteins (Yang et al. 2017). As an ATP-independent molecular chaperone, HSP20 resists various stresses, including oxidative stress, by reconstructing normal protein conformation and intracellular homeostasis. H_2O_2-induced differential HSP20 protein balances ROS concentration by protecting the activity of ROS-scavenging proteins, thereby regulating fruit development (Yu et al. 2016). During banana ripening, reactive oxygen stress leads to the oxidation of proteins containing thiols to regulate fruit ripening, and the expression of HSP20s protein is

Downloaded from https://academic.oup.com/plphys/article/201/3/kiag454/8721702 by Uladag University user on 14 July 2026

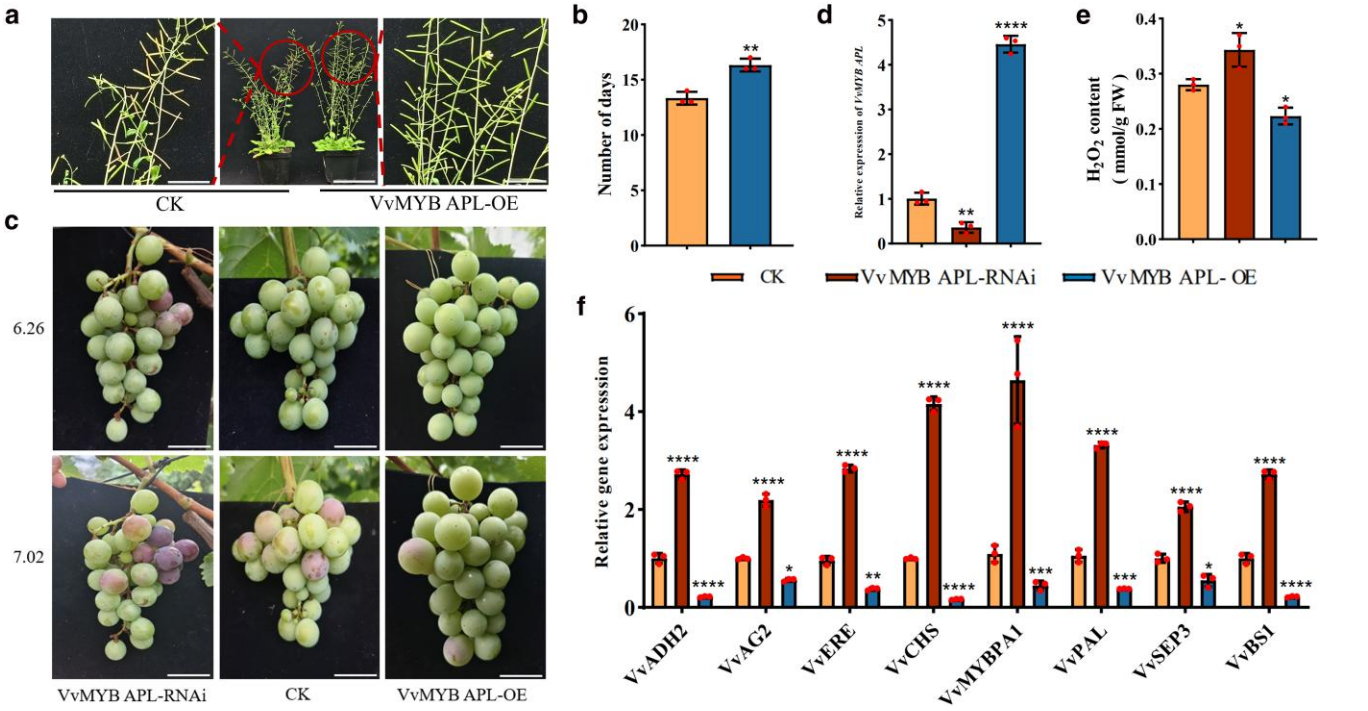


Figure 5 *VvMYB APL* negatively regulates fruit ripening. a) Phenotypic observation of positive transgenic *Arabidopsis* plants expressing *VvMYB APL*. CK: wild type plants serve as a control. Scale bar is 1 cm. b) The mature days of *Arabidopsis* fruit pods. Data are presented as means ± SD of 3 independent biological replicates ($n = 3$), representing 3 independent transgenic lines. c) Grape berry phenotypes transiently overexpressing or silencing *VvMYB APL*. CK: pIR empty as control. Scale bar is 1 cm. d) The expression pattern of *VvMYB APL* in transgenic berries. Three independent biological replicates were analyzed for each treatment, and each biological replicate was measured using 3 technical PCR replicates. Data are presented as mean ± SD. e) Analysis of H_2O_2 content of *VvMYB APL* in transgenic berries. FW, fresh weight. Data are presented as means ± SD of 3 independent biological replicates ($n = 3$). Each biological replicate consists of 3 grape clusters processed independently. f) Expression patterns of ripening-related genes in transgenic berries. Three independent biological replicates were analyzed for each treatment, and each biological replicate was measured using 3 technical PCR replicates. Data are presented as mean ± SD. Data in b), d) and e) were analyzed by one-way ANOVA; data in f) was analyzed by two-way ANOVA. Significant differences were observed between the treatment group and the control group (*$0.01 < P < 0.05$, $0.001 <$ **$P < 0.01$, $0.0001 <$ ***$P < 0.001$, ****$P < 0.0001$). All *P*-values are shown in Data Set S2.

upregulated. In tomato, chloroplast HSP21 protects plant photosystem II from temperature-dependent oxygen stress and plays a key role in the transformation of chloroplasts to pigment cells during tomato fruit ripening (Neta-Sharir et al. 2005). Silencing of *SlHSP17.7* by RNA interference delayed fruit ripening (Liu et al. 2023). In this study, overexpression of *VvHSP20-43* significantly inhibited *Arabidopsis* development, especially flowering and podding. And the transient transformation of *VvHSP20-43* in grape berries confirmed that it could inhibit fruit ripening. The above results suggest that HSP20s should play an important role during fruit ripening.

Fruit ripening involves strong internal transcription and biochemical modification, which is the result of the interaction of multiple genes (Tang et al. 2020). The function of the HSP20 protein in plant development, especially the response to ROS, is regulated by a series of transcription factors (Ji et al. 2019). Based on the co-expression network analysis of grape microarray and transcriptome data (Wong 2020), MYB APL was considered to be an interacting protein of HSP20. In this work, *VvMYB APL* has been shown to play a negative regulatory role in grape berry ripening. In *Arabidopsis*, MYB APL is involved in the regulation of flower development. In previous studies, the important functions of MYB transcription factors in fruit development and ripening were described in detail, including the response to ROS. In fruit, the effect of ROS on gene expression depends on redox-sensitive transcription factors. In *Arabidopsis*, ROS-responsive *AtMYB30* is essential for root growth regulation during defense responses (Mabuchi et al. 2018). Overexpression of banana *BnaMYB111L* in tobacco and rapeseed protoplasts promoted reactive oxygen species production and hypersensitivity-like cell death (Yao et al. 2020). These results indicate that MYB transcription factors are closely related to ROS response. More importantly, in this study, through multidatabase joint prediction, co-expression network analysis, and experimental validation, we identified VvMYB APL as the key transcription factor regulating *VvHSP20-43* expression. Yeast one-hybrid, dual luciferase reporter systems, and EMSA experiments all confirmed that VvMYB APL can directly bind to the *VvHSP20-43* promoter and activate its transcription. This provides a molecular link for understanding ROS signaling and the *HSP20* gene.

Fruit ripening is a highly coordinated physiological process involving complex interactions between hormones, transcription factors, and reactive oxygen species signaling. In addition, a major characteristic of fruit ripening is the accumulation of H_2O_2. H_2O_2, as a signal molecule, can mediate the oxidative modification of proteins. Similar to other types of protein post-translational modifications such as ubiquitination, phosphorylation, and acetylation (Jiang et al. 2018), H_2O_2 oxidative modification can change the subcellular localization of proteins, protein-protein interactions, and protein biological activity and stability at multiple levels, thereby changing protein function to regulate the growth and development of organisms and

Downloaded from https://academic.oup.com/plphys/article/201/3/kiag454/8721702 by Uladag University user on 14 July 2026

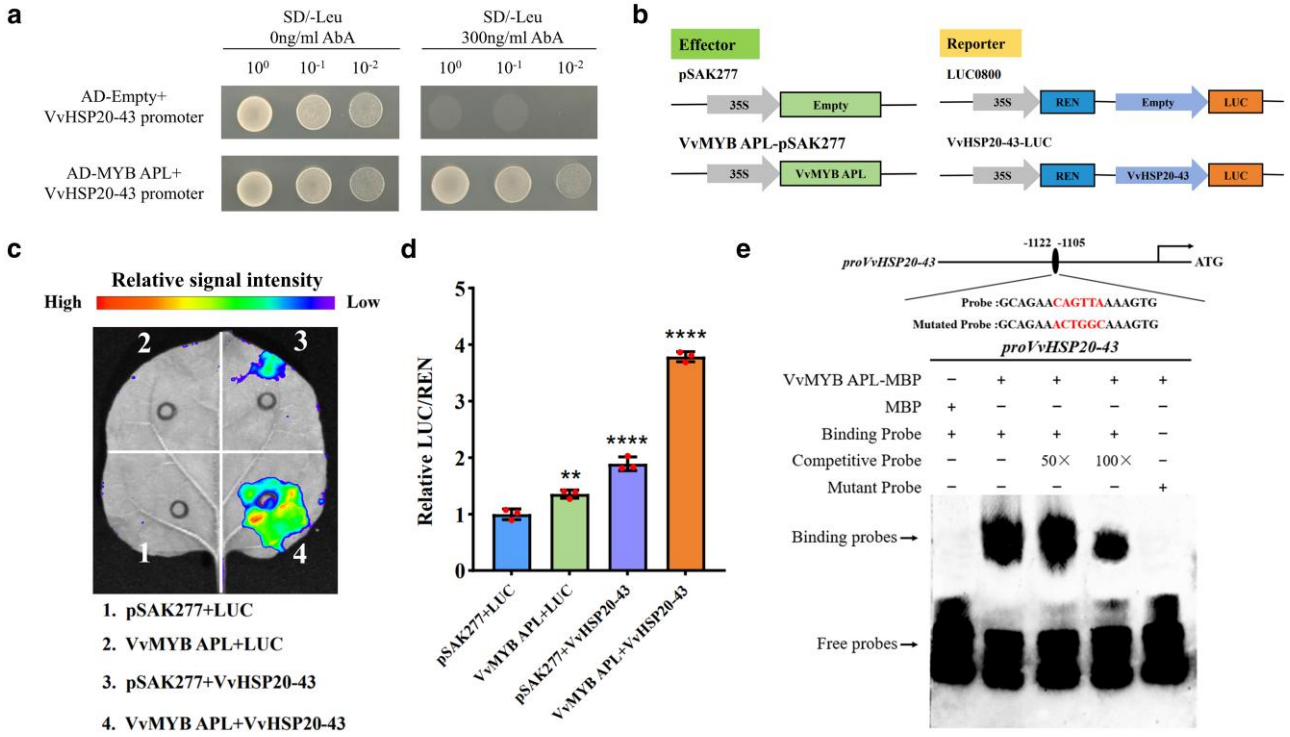


Figure 6 Verification of interaction between VvHSP20-43 promoter and VvMYB APL. a) Yeast one-hybrid test. Yeast cells were cotransformed with prey AD-VvMYB APL and bait constructed from the *proVvHSP20-43*-pAbAi fragment on SD/-Leu and SD/-Leu selective medium containing 300 ng/mL AbA. b) Schematic diagram of the vectors for the dual luciferase reporter assay. c) Transient expression assay showing that VvMYB APL activates *VvHSP20-43* transcriptional expression. d) Dual-luciferase assay demonstrated that VvMYB APL promotes the transcriptional expression of *VvHSP20-43*. Three biological replicates were performed for the dual-luciferase reporter assay. Each biological replicate was derived from 3 tobacco plants. Data are presented as mean ± SD. e) EMSA showing that the VvMYB APL protein binds directly to the *VvHSP20-43* promoter. Data in d) was analyzed by one-way ANOVA; significant differences were observed between the treatment group and the control group (*$0.01 < P < 0.05$, $0.001 <$ **$P < 0.01$, $0.0001 <$ ***$P < 0.001$, ****$P < 0.0001$). All *P*-values are shown in Data Set S2.

response to stress (Liu et al. 2019). The reversible redox modification of Cys and Met residues acts as a switch to conduct signals. For example, reversible oxidative modification of brassinosteroid signaling factor BZR1 can link H_2O_2-mediated redox signaling to regulate plant development (Liu et al. 2019). Through sequence analysis, multiple Met oxidation sites were confirmed to exist in the VvMYB APL protein. Proteins rich in Met domains are easily oxidized by ROS, and the oxidation of Met affects the interaction between genes and target proteins. This study elucidates the molecular mechanism by which H_2O_2 regulates grape berry ripening through the oxidative modification of the transcription factor VvMYB APL, which subsequently modulates the expression of its downstream target gene *VvHSP20-43* (Fig. 8). This discovery extends our understanding of ROS signaling mechanisms in nonclimacteric fruits and provides insights into the post-transcriptional regulatory networks governing fruit ripening.

Conclusions

This study establishes that H_2O_2 accelerates grape ripening by oxidizing the transcription factor VvMYB APL, impairing its binding to the *VvHSP20-43* promoter and repressing *VvHSP20-43* expression. Transgenic studies confirm that both *VvMYB APL* and *VvHSP20-43* act as negative regulators of ripening. Our results thus unveil a redox-mediated transcriptional pathway in grape berry ripening, providing a mechanistic link between ROS signaling and ripening regulation in grapes.

Materials and methods

Plant materials

The grape berry plant material used for RNA and DNA extraction and transgenic in this study was derived from berries from the cultivar "Kyoho", growing under natural cultivation conditions in the experimental field of Henan University of Science and Technology (Henan, China). The methods for obtaining grape berry materials at K1, K2, K3, K4, K5, and K6 periods referred to the experimental methods of Wei et al. (2025). Harvested grape berries were frozen in a −80°C ultra-low temperature refrigerator. *Arabidopsis* and *Nicotiana benthamiana* for *Agrobacterium*-mediated stable transformations and transient transformations were obtained from seeds preserved by our research group.

Extraction of DNA and RNA and synthesis of cDNA

Total RNA of grape berry tissues was extracted using the RNAprep Pure Plant Plus Kit (Polysaccharides & Polyphenolics-rich) (DP441) of Tiangen Biochemical Technology Co., Ltd. (Beijing, China). The cDNA was obtained by reverse transcription of total RNA using the HiFi Script cDNA Synthesis Kit of Beijing Kangwei Biological Co., Ltd. (Beijing, China). DNA of grape berries was extracted using the FastPure Plant DNA Isolation Mini kit-BOX2 (DC104-01) (Vazyme, Nanjing, China) DNA extraction Kit of Vazyme Biotechnology Co., Ltd. Refer to the kit instructions for specific parameters.

Downloaded from https://academic.oup.com/plphys/article/201/3/kiag454/8721702 by Uladag University user on 14 July 2026

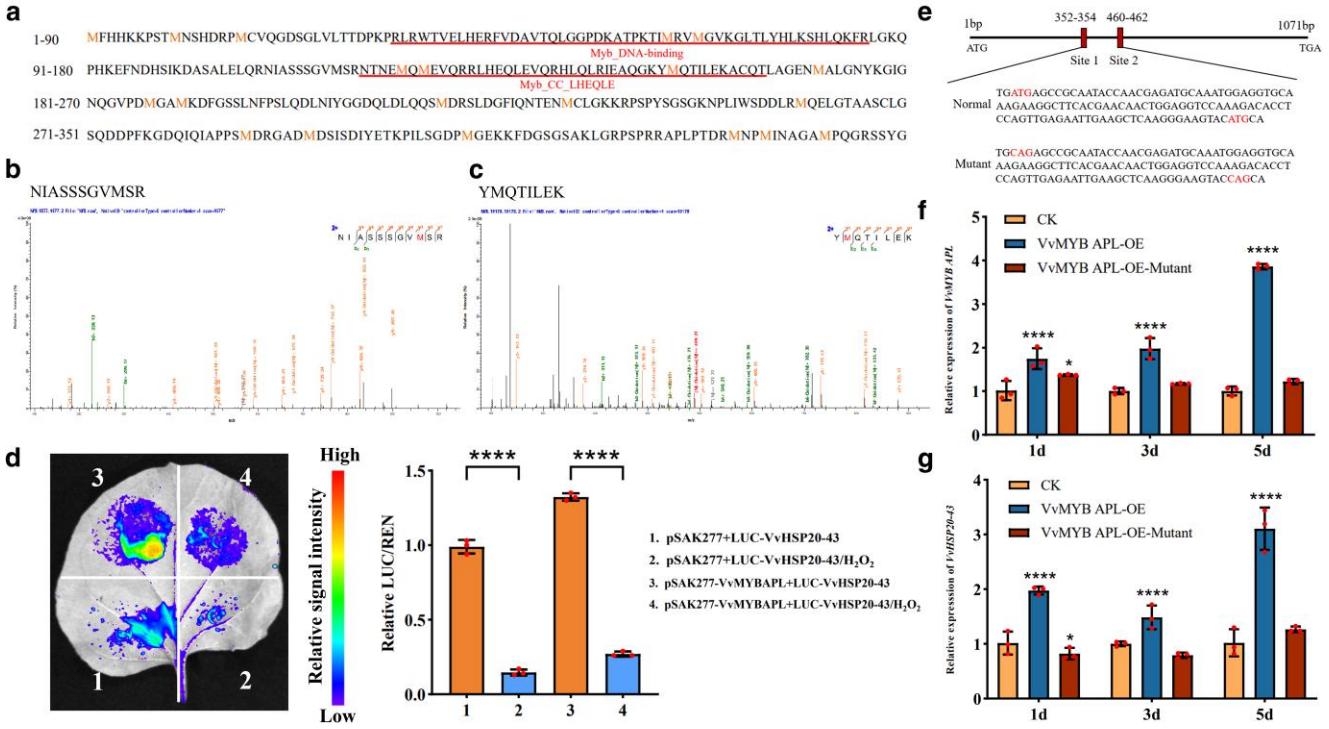


Figure 7 Identification of the oxidation sites in the VvMYB APL protein and verification of the regulatory relationship between VvMYB APL and the *VvHSP20-43* promoter under H_2O_2 treatment. a) Amino acid sequence analysis of VvMYB APL protein. b) Identification of the first Met oxidation sites of VvMYB APL protein after H_2O_2 treatment. c) Identification of the second Met oxidation sites of VvMYB APL protein after H_2O_2 treatment. d) H_2O_2 treatment reduces the activation of the *VvHSP20-43* promoter by VvMYB APL. Three biological replicates were performed for the dual-luciferase reporter assay. Each biological replicate was derived from 3 tobacco plants. Data are presented as mean ± SD. e) Schematic diagram of the normal and mutant sequences of the CDS region in *VvMYB APL*. f) RT-qPCR assay for relative expression of the *VvMYB APL*. CK: overexpression empty vector. Data are presented as mean ± SD. g) RT-qPCR assay for relative expression of the *VvHSP20-43.* Samples of grape fruit were collected at 1 d, 3 days, and 5 days. Three independent biological replicates were analyzed for each treatment, and each biological replicate was measured using 3 technical PCR replicates. CK: overexpression empty vector. Data are presented as mean ± SD. Data in d) were analyzed by one-way ANOVA; data in f) and g) were analyzed by two-way ANOVA. Significant differences were observed between the treatment group and the control group (*$0.01 < P < 0.05$, $0.001 <$ **$P < 0.01$, $0.0001 <$ ***$P < 0.001$, ****$P < 0.0001$). All *P*-values are shown in Data Set S2.

Gene cloning and sequence analysis

CDS and amino acid sequences of grape *VvHSP20-43* and *VvMYB APL* genes were obtained from the Ensembl Plants database. Primers were designed using Primer Premier 5.0 software, and the berry cDNA was used as the amplification template for PCR with the high-fidelity enzyme 2×Key Phanta Max Master Mix program. PCR products were sequenced by Sanger technology provided by Shenggong BioEngineering (Zhengzhou, China). The sequence obtained by sequencing was compared with the sequence in the Ensembl Plants database to confirm that no base mismatch was submitted to MEME to predict its motif (https://meme-suite.org/meme/). The conserved domain was predicted by the SMART website (https://smart.embl.de), and the sequence was blasted in the UniProt database. HSP20 proteins of 5 species with high homology were selected, and the phylogenetic tree was constructed based on the MEGA7.0 N-J method.

Analysis of promoter activity

The 2,000 bp sequences upstream of *VvHSP20-43* and *VvMYB APL* gene transcription start sites were used as promoters, and primers were designed by Premier 5.0 software. Using the DNA in "Kyoho" fruit as an amplification template, PCRs were carried out, and the PCR products were further sequenced by Sanger technology. The correctly sequenced promoter sequences are used for cis-acting element prediction at the PlantCARE online tools. The primers used in this assay are shown in Data Set S1.

Suitable with the instructions for the Seamless Cloning Kit (Shanghai, China) produced by Biyuntien, the cloned *VvHSP20-43* gene promoter fragment was connected with the 0390-GUS vector by DNA ligase and then transferred to the DH5α receptor state of the large colon. Positive clones were screened by PCR and sequencing. The recombinant plasmid of the positive strain was extracted, and the recombinant plasmid and empty plasmid were respectively introduced into the *Agrobacterium tumefaciens* GV3101 strain (Weidibio, Shanghai, China).

The isolated tobacco and grape leaves were immersed in *Agrobacterium* solution resuspension under the distal axis and then vacuum permeated. Osmotic solution was used for negative control, and 35S-GUS was used for positive control. The leaves were cultured at 25 ℃, 16:8 light and dark conditions for 24 h and then treated with 300 mmol/L H_2O_2 solution and cultured for 24 h. At the end of the culture, the tobacco leaves were dyed according to the GUS Blue kit instructions, cultured at 37 ℃ for 12–24 h, and then decolourized with 75% alcohol.

Subcellular localization

The cloned gene fragments of *VvHSP20-43* and *VvMYB APL* were cloned into the 101L YFP vector via restriction ligation of *Eco*R I and

Downloaded from https://academic.oup.com/plphys/article/201/3/kiag454/8721702 by Uladag University user on 14 July 2026

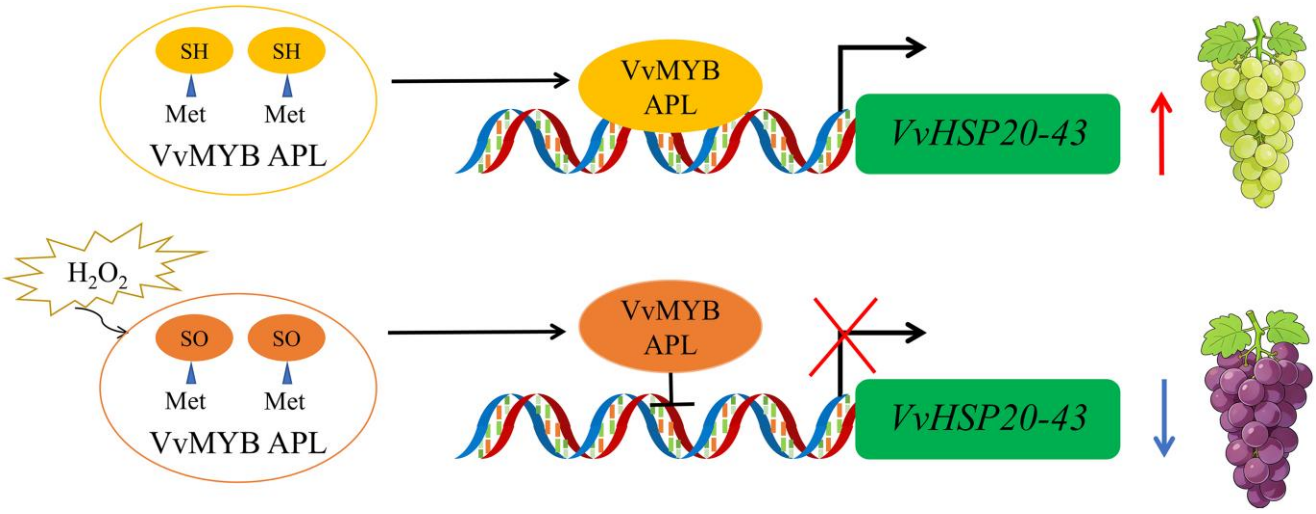


Figure 8 Mechanism of H_2O_2 treatment regulating grape berry ripening. Under normal conditions, the VvMYB APL protein is expressed normally and can specifically bind to the *VvHSP20-43* promoter, activating the transcriptional expression of *VvHSP20-43* and delaying grape berry ripening. Under H_2O_2 treatment, Met residues in the VvMYB APL protein are oxidized to Met sulfate. This oxidation prevents VvMYB APL from binding to the *VvHSP20-43* promoter region, ultimately promoting berry ripening.

*Bam*H I sites, and then transformed into *E. coli* (DH5α). After successful sequencing, the recombinant plasmid was transformed into *Agrobacterium tumefaciens* GV3101 strain. The recombinant plasmids and a YFP control were mixed in proportion with cytoplasmic markers (or nuclear markers) and p19 helper plasmids, respectively. Transient expression was performed by infiltrating tobacco (*Nicotiana benthamiana*) leaves with a 1-mL syringe. After infiltration, the infected tobacco plants were cultured in dark for 12 h and then cultured in low light for 48 h. The leaves were cut, and the fluorescence signals were observed under a confocal laser scanning microscope. The primers used in this assay are shown in Data Set S1.

Prediction of transcription factors and GO enrichment analysis

According to the promoter sequence of *VvHSP20-43*, the CIS-BP database was used to predict potential TFs. And the information of TFs in grapes was obtained based on PlantTF-BP and annotated using BLAST. FIMO was used to scan transcription factor binding sites in the *VvHSP20-43* promoter, with 10^{-5} as the threshold. In addition, based on Plant TF Binding Motif Shift and Fimo Binding Site Scan, the potential TFs in the *VvHSP20-43* promoter region were predicted. The above results were analyzed by a Veen diagram. The obtained candidate transcription factors were subjected to GO annotation analysis. In addition, the binding sites of *VvHSP20-43* to candidate TFs were identified based on AlphaFold3 (https://alphafoldserver.com/).

Stable genetic transformation mediated by *agrobacterium*

The CDS sequences of cloned *VvHSP20-43* and *VvMYB APL* were cloned into the pCAMBIA2300-GFP vector via restriction ligation with the *Bam*H I enzyme, and then transformed into *E. coli* (DH5α). After successful sequencing, recombinant plasmids of positive strains were extracted, and the recombinant plasmids were transferred to *Agrobacterium tumefaciens* GV3101 strain. The inflorescence of *Arabidopsis thaliana* was infected by the floral dip method. The flower buds of *Arabidopsis thaliana* were infected in a centrifuge tube containing the inflorescence solution for 10 min, then cultured in the dark for 24 h, and then cultured under normal light. The primers used in this assay are shown in Data Set S1.

Transient transgenic of grape berries

Viral vector pIR was constructed and transfected according to the method of Peretz et al. (2007). To construct *VvHSP20-43* and *VvMYB APL* overexpression vectors, the CDS sequences of *VvHSP20-43* and *VvMYB APL* were subcloned into the pIR-GUS vector by double enzyme restriction of *Bam*H I and *Xba* I, respectively, replacing the *GUS* coding gene. The resulting structures are named pIR-*VvHSP20-43*-OE and pIR-*VvMYB APL*-OE. Similarly, the CDS sequences of *VvHSP20-43* and *VvMYB APL* were reverse-subcloned into the pIR-GUS vector, respectively, to replace the *GUS* coding gene, and the resulting constructs were named pIR-*VvHSP20-43*-RNAi and pIR-*VvMYB APL*-RNAi. The 4 constructs were transformed into DH5α cells and extracted from overnight cultures. The primers used in this assay are shown in Data Set S1.

The transient transformation of grape berries was conducted in the field via capillary-based injection of the vectors into grape bunch tissue. This method is described briefly here. Grape berries grown under natural cultivation conditions approximately 30 DAF were selected. Approximately 200 ng of plasmid DNA (OE or RNAi) was injected into a capillary tube together with the IL-60-BS auxiliary carrier plasmid. Capillary tubes were then inserted into the stalk of the grape cluster, and plasmid DNA was allowed to transfer into the grape fruits via capillary tube action. For each bunch, 2 injections were performed 1 wk apart. Grape samples were collected prior to transformation, 3 days after the transformation, and at the late-ripening stage. One biological replicate includes 3 clusters. After treatment, the berries with similar directions and locations in different clusters were sampled from the clusters with uniform development, ensuring that the selected fruits have consistent ripeness for subsequent analysis, and then were subsequently stored at −80 °C for physiological measurements and quantitative analysis.

Downloaded from https://academic.oup.com/plphys/article/201/3/kiag454/8721702 by Uladag University user on 14 July 2026

Gene expression analysis

The fluorescence quantitative primers of *VvHSP20-43*, *VvMYB APL*, *VvERE*, *VvCHS*, *VvPAL*, *VvMYBPA1*, *VvBS1*, *VvADH2*, *VvAG2*, and *VvSEP3* genes were designed using Primer Blast from the NCBI online website. RNA was extracted from transiently transformed grape berry tissues and converted to cDNA as described above. Quantitative real-time PCR (qPCR) was performed using the Cham QTM Universal SYBR qPCR Master Mix (Vazyme, Nanjing, China) and Quantagene q225 fluorescent quantitative PCR instrument (Beijing, China). Sample analysis was repeated in triplicate in all experiments, using the reference gene, Ubiquitin, to normalize the expression level of the detected gene according to the $2^{-\Delta\Delta CT}$ algorithm. The primers used in this assay are shown in Data Set S1.

Determination of H_2O_2 content in grape berries

H_2O_2 content in grape berries was determined according to the hydrogen peroxide test kit of Nanjing Jiancheng Bioengineering Institute (Nanjing, China). Grape berry samples were ground with liquid nitrogen; according to the ratio of weight (g) to volume (mL) = 1:9, 0.1 g of the sample was weighed and dissolved in 0.9 mL of PBS solution, vortex oscillated and centrifuged, and the supernatant was taken to be measured. The specific determination method shall be carried out in accordance with the instructions of the hydrogen peroxide test kit. Three biological replicates were performed for each sample, each consisting of a mixture of berries from 3 clusters.

Anthocyanin and sucrose content determination

The anthocyanin content in the samples was determined using the pH differential method. Approximately 0.5 g of grape berries were ground in liquid nitrogen, then 2 mL of 1% HCl-methanol extraction solution was added, and the mixture was sonicated for 30 min at low temperature in the dark. After centrifugation, the supernatant was collected and diluted 10-fold with KCl buffer (pH 1.0) and d $CH_3CO_2Na{\cdot}3H_2O$ buffer (pH 4.5), respectively. The absorbance values of each treated solution were measured at wavelengths of 520 and 700 nm using a UV-visible spectrophotometer. Three biological replicates were used for each treatment.

Sucrose content was determined using the resorcinol-hydrochloric acid method. Briefly, 0.5 g of fresh tissue was ground and extracted with 5 mL of distilled water in a boiling water bath for 30 min. The extract was filtered, transferred to a 25 mL volumetric flask, and brought to volume with distilled water. Then, 0.4 mL of the extract was mixed with 200 μL of 2 mol/L NaOH and hydrolyzed at 100 °C for 5 min. After cooling, 2.8 mL of 30% HCl and 0.8 mL of 0.1% resorcinol solution were added, and the mixture was incubated at 80 °C for 10 min for color development. Deionized water was used as the blank control, and the absorbance was measured at 480 nm. The sucrose standard curve equation was $y = 0.003x + 0.018$, where y represents the absorbance and x represents the sugar content (μg). The sugar content in the samples was calculated according to the standard curve, and sucrose content was then calculated using the following formula: Sucrose content $(mg/g) = (C \times V \times n)/(W \times a \times 10^3)$. Three biological replicates were used for each treatment, each consisting of a mixture of berries from the 3 clusters.

Yeast one-hybrid assay

The promoter sequence of *VvHSP20-43* was cloned into the pBait-AbAi vector. The construct was linearized into the Y1H GOLD yeast strain and coated in SD/-Ura-deficient medium to screen for appropriate aurobasidium A (AbA) concentration. The CDS sequence of *VvMYB APL* was cloned into the pGADT7 vector. AD-VvMYB APL was incorporated into the yeast containing pBait-AbAi-*VvHSP20-43* and coated on SD/Leu medium. Finally, the conversion results were identified by SD/-Leu AbA medium with AbA concentration screening. The primers used in this assay are shown in Data Set S1.

Dual-luciferase reporter assay

The *VvHSP20-43* promoter was cloned into the pGreenII-0800-LUC vector via restriction ligation with *Hind* III and *Bam*H I. The CDS sequence of *VvMYB APL* gene was cloned into the pSAK277 vector digested with *EcoR* I. The constructed effector plasmid and reporter plasmid were transferred into the *Agrobacterium tumefaciens* GV3101 strain and then infiltrated into tobacco (*Nicotiana benthamiana*) leaves. The primers used in this assay are shown in Data Set S1.

Leaves from 4 to 6-wk-old tobacco plants were selected as explants, and the agrobacteria containing the recombinant plasmids containing the *VvMYB APL* transcription factor and *VvHSP20-43* promoter were suspended in the induction solution in a ratio of 9:1. The suspension was then injected into the underside of the tobacco leaf through a syringe for transient expression. After infiltration the tobacco plants were cultured in the dark for 12 h and then cultured in the low light for 2 days. Experimental plants were treated with a 300 mM H_2O_2 solution to test the effect of H_2O_2 on the interaction of VvMYB APL and *VvHSP20-43*. Firefly luciferase (LUC) and renal luciferase (REN) activities were measured using a dual luciferase report assay kit, and the final transcriptional activity was reflected by calculating the ratio of LUC to REN fluorescence. Fluorescence was measured with the NightOWL II LB 983 live imaging system from Berthold (CN)-Berthold Technologies GmbH.

Protein purification

The CDS sequences of *VvMYB APL* were inserted into the pMAL-c6T vector and transferred into the DH5α receptor strain. After successful sequencing, the plasmid was extracted and transferred into the *Escherichia coli* BL21(DE3) strain. The expression of the *VvMYB APL* protein was induced by IPTG, and the target protein was purified by an affinity column after cell fragmentation. The expression of the target protein and the purity of the purified protein were detected by SDS-PAGE (see the NEBExpress MBP Fusion and Purification System kit manual for details). The primers used in this assay are shown in Data Set S1.

LC-MS/MS analysis to identify the oxidation site of VvMYB APL protein

The purified VvMYB APL protein was treated with a 1 mM H_2O_2 solution, and the site of H_2O_2 oxidation modification of the VvMYB APL protein was identified by the LC-MS/MS system. In the LC-MS/MS system, the isolated VvMYB APL protein molecules are first ionized and measured in the mass spectrometer MS1, followed by the ion fragmentation and further analysis in the mass spectrometer MS2. According to the electrical signal generated by the ionization of the MYB APL protein, the mass spectrum peak is further processed by

Downloaded from https://academic.oup.com/plphys/article/201/3/kiag454/8721702 by Uladag University user on 14 July 2026

computer data and then analyzed and annotated. The work is completed by Shanghai Baipu Biotechnology Co., Ltd. (Shanghai, China).

Electrophoretic mobility shift assay

The coding sequence of *VvMYB APL* was cloned into the pET-28a expression vector to enable prokaryotic expression of the recombinant VvMYB APL protein tagged with MBP. Biotin-labeled probes containing Myb elements, along with their mutated versions from the *VvHSP20-43* promoter, were used, with unlabeled probes acting as competitors for binding. An EMSA was performed to examine the interaction between the purified VvMYB APL protein and these probes. The specific primers and probes used in this experiment are listed in Data Set S1.

Statistical analysis

All real-time PCR and other quantitative experiments were performed a minimum of 3 times. Three technical PCR replicates were performed for each biological replicate. One-way ANOVA was utilized to evaluate the variation in the dependent variable caused by 1 independent variable. Two-way ANOVA was applied to examine the distinct effects of 2 independent variables on the dependent variable. For multiple comparisons, significance was determined using one-way and two-way ANOVA followed by Tukey's multiple comparison tests. The statistical analysis was performed using GraphPad Prism software (version 9.0) by entering the raw data. Statistical data are provided in Data Set S2.

Accession numbers

Sequence data from this article can be found in the GenBank/EMBL data libraries under accession numbers: *VvHSP20-43* (Vitvi19g00403), *VvMYB APL* (Vitvi19g01742), *VvADH2* (Vitvi04g01669), *VvAG2* (Accession No: TC62522), *VvERE* (Accession No: TT282A08), *VvCHS* (Vitvi05g01044), *VvMYBPA1* (Vitvi15g00938), *VvPAL* (Accession No: CX127428), *VvSEP3* (Accession No: AF373603), *VvBS1* (Locus Tag: GSVIVT00031869001).

Acknowledgments

We thank the following colleagues for their help and expertise: Hui-Ying Jin for measuring physiological parameters, Guang-Qi He and Yong-Ke Wu for measuring gene expression.

Author contributions

D.-L.G. planned and designed the research. J.-L.X. and L.Y. performed the experiments, collected and analyzed the data, and wrote the manuscript draft. D.-D.Z. participated in the production of some pictures of the thesis. R.-Y.L., J.Z., M.-L.Z., H.-N.L., M.-S.P., and T.-L.W. provided experimental guidance. J.G.L. and A.A. finalized the revision of the manuscript. All authors have read and approved the final version of the manuscript.

Supplementary material

Supplementary material is available at *Plant Physiology* online.

Funding

This work was financially supported by the Natural Science Foundation of Henan Province (232300421112) and the National Natural Science Foundation of China (NSFC: 32472662).

Conflicts of interest

None declared.

Data availability

The data underlying this article are available in the article and in its online supplementary material.

References

Almanza-Oliveros A *et al.* 2024. Grape pomace—advances in its bioactivity, health benefits, and food applications. *Foods*. 13:580. https://doi.org/10.3390/foods13040580.

Arce D *et al.* 2016. Heterogeneous expression pattern of tandem duplicated sHsps genes during fruit ripening in two tomato species. *J Phys Conf Ser*. 705:012004. https://doi.org/10.1088/1742-6596/705/1/012004.

Atak A. 2024. Challenges and strategies for table grape breeding in the face of global climate change. *Acta Hortic.* 1401:33–40. https://doi.org/10.17660/ActaHortic.2024.1401.5.

Atak A, Akgün M, Şen A, Göksel Z, Uzun A. 2025. Evaluation of quality characteristics and cultivar candidate potentials of hybrid genotypes obtained from different Vitis species. *Horticulturae*. 11:354. https://doi.org/10.3390/horticulturae11040354.

Di Genova A *et al.* 2014. Whole genome comparison between table and wine grapes reveals a comprehensive catalog of structural variants. *BMC Plant Biol*. 14:1–12. https://doi.org/10.1186/1471-2229-14-7.

Guo DL *et al.* 2019. Hydrogen peroxide treatment promotes early ripening of kyoho grape. *Aust J Grape Wine R*. 25:357–362. https://doi.org/10.1111/ajgw.12399.

Guo D-L, Wang Z-G, Pei M-S, Guo L-L, Yu Y-H. 2020. Transcriptome analysis reveals mechanism of early ripening in kyoho grape with hydrogen peroxide treatment. *BMC Genomics*. 21:1–18. https://doi.org/10.1186/s12864-020-07180-y.

Ji X-R, Yu Y-H, Ni P-Y, Zhang G-H, Guo D-L. 2019. Genome-wide identification of small heat-shock protein (HSP20) gene family in grape and expression profile during berry development. *BMC Plant Biol*. 19:1–15. https://doi.org/10.1186/s12870-019-2031-4.

Jiang G *et al.* 2018. Sulfoxidation regulation of Musa acuminata calmodulin (MaCaM) influences the functions of MaCaM-binding proteins. *Plant Cell Physiol*. 59:1214–1224. https://doi.org/10.1093/pcp/pcy057.

Jiang G *et al.* 2020. Redox regulation of the NOR transcription factor is involved in the regulation of fruit ripening in tomato. *Plant Physiol*. 183:671–685. https://doi.org/10.1104/pp.20.00070.

Jin W *et al.* 2016. The R2R3 MYB transcription factor PavMYB10.1 involves in anthocyanin biosynthesis and determines fruit skin colour in sweet cherry (*Prunus avium* L.). *Plant Biotechnol J*. 14:2120–2133. https://doi.org/10.1111/pbi.12568.

Kumar V *et al.* 2016. Fruit ripening mutants reveal cell metabolism and redox state during ripening. *Protoplasma*. 253:581–594. https://doi.org/10.1007/s00709-015-0836-z.

Liao W-B, Huang G-B, Yu J-H, Zhang M-L. 2012. Nitric oxide and hydrogen peroxide alleviate drought stress in marigold explants and promote its adventitious root development. *Plant Physiol Biochem*. 58:6–15. https://doi.org/10.1016/j.plaphy.2012.06.012.

Downloaded from https://academic.oup.com/plphys/article/201/3/kiag454/8721702 by Uladag University user on 14 July 2026

Liu C, Yu H, Li L. 2019. SUMO modification of LBD30 by SIZ1 regulates secondary cell wall formation in *Arabidopsis thaliana*. *PLoS Genet*. 15: e1007928. https://doi.org/10.1371/journal.pgen.1007928.

Liu W *et al.* 2023. RNA interference-induced silencing of the *SlHSP17.7* gene delays fruit ripening in tomato. *J Plant Biochem Biotechnol*. 32:153–162. https://doi.org/10.1007/s13562-022-00790-5.

Mabuchi K *et al.* 2018. MYB30 links ROS signaling, root cell elongation, and plant immune responses. *Proc Natl Acad Sci U S A*. 115:E4710–E4719. https://doi.org/10.1073/pnas.1804233115.

Neta-Sharir I, Isaacson T, Lurie S, Weiss D. 2005. Dual role for tomato heat shock protein 21: protecting photosystem II from oxidative stress and promoting colour changes during fruit ripening. *Plant Cell*. 17: 1829–1838. https://doi.org/10.1105/tpc.105.031914.

Peretz Y *et al.* 2007. A universal expression/silencing vector in plants. *Plant Physiol*. 145:1251–1263. https://doi.org/10.1104/pp.107.108217.

Quan L-J, Zhang B, Shi W-W, Li H-Y. 2008. Hydrogen peroxide in plants: a versatile molecule of the reactive oxygen species network. *J Integr Plant Biol*. 50:2–18. https://doi.org/10.1111/j.1744-7909.2007.00599.x.

Segade SR *et al.* 2013. Impact of different advanced ripening stages on berry texture properties of 'red globe' and 'crimson seedless' table grape cultivars (*Vitis vinifera* L.). *Sci Hortic*. 160:313–319. https://doi.org/10.1016/j.scienta.2013.06.017.

Steelheart C *et al.* 2022. High light stress induces H_2O_2 production and accelerates fruit ripening in tomato. *Plant Sci*. 322:111348. https://doi.org/10.1016/j.plantsci.2022.111348.

Tang D, Gallusci P, Lang Z. 2020. Fruit development and epigenetic modifications. *New Phytol*. 228:839–844. https://doi.org/10.1111/nph.16724.

Torres-Palazzolo C *et al.* 2024. Recent advances in biocontrol and other alternative strategies for the management of postharvest decay in table grapes. *Int J Food Microbiol*. 420:110766. https://doi.org/10.1016/j.ijfoodmicro.2024.110766.

van Montfort RL, Basha E, Friedrich KL, Slingsby C, Vierling E. 2001. Crystal structure and assembly of a eukaryotic small heat shock protein. *Nat Struct Biol*. 8:1025–1030. https://doi.org/10.1038/nsb722.

Wang P *et al.* 2021. Redox proteomic analysis reveals the involvement of oxidative post-translational modification in tomato fruit ripening. *Postharvest Biol Tec*. 178:111556. https://doi.org/10.1016/j.postharvbio.2021.111556.

Wei T-L *et al.* 2025. CHH hypermethylation contributes to the early ripening of grapes revealed by DNA methylome landscape of 'kyoho' and its bud mutant. *Hortic Res*. 12:uhae285. https://doi.org/10.1093/hr/uhae285.

Wong DCJ. 2020. Network aggregation improves gene function prediction of grapevine gene co-expression networks. *Plant Mol Biol*. 103:425–441. https://doi.org/10.1007/s11103-020-01001-2.

Yang L, Zuo DD, Guo DL. 2025. The role of hydrogen peroxide in fruit ripening regulation. *J Plant Growth Regul*. 44:3375–3387. https://doi.org/10.1007/s00344-025-11630-w.

Yang M *et al.* 2017. Identification of MsHsp20 gene family in *Malus sieversii* and functional characterization of MsHsp16. 9 in heat tolerance. *Front Plant Sci*. 8:1761. https://doi.org/10.3389/fpls.2017.01761.

Yao L *et al.* 2020. The R2R3-MYB transcription factor BnaMYB111L from rapeseed modulates reactive oxygen species accumulation and hypersensitive-like cell death. *Plant Physiol Biochem*. 147:280–288. https://doi.org/10.1016/j.plaphy.2019.12.027.

Yu J *et al.* 2016. Genome-wide identification and expression profiling of tomato *Hsp20* gene family in response to biotic and abiotic stresses. *Front Plant Sci*. 7:1215. https://doi.org/10.3389/fpls.2016.01215.

Zhu L *et al.* 2023. Methionine oxidation and reduction of the ethylene signaling component MaEIL9 are involved in banana fruit ripening. *J Integr Plant Biol*. 65:150–166. https://doi.org/10.1111/jipb.13363.

Zuo D-D *et al.* 2024. Hydrogen peroxide priming triggers splicing memory in grape berries. *Plant Mol Biol*. 114:129. https://doi.org/10.1007/s11103-024-01528-8.

Zuo D-D *et al.* 2025. Histone H3K4 demethyltransferase VvJMJ14 promotes H_2O_2 inducing fruit ripening in grape. *Plant J*. 124:e70642. https://doi.org/10.1111/tpj.70642.

Downloaded from https://academic.oup.com/plphys/article/201/3/kiag454/8721702 by Uladag University user on 14 July 2026